



Two-Gap Superconductivity in LaNiGa_2 with Nonunitary Triplet Pairing and Even Parity Gap Symmetry

Z. F. Weng,¹ J. L. Zhang,¹ M. Smidman,^{1,*} T. Shang,¹ J. Quintanilla,² J. F. Annett,³ M. Nicklas,⁴ G. M. Pang,¹ L. Jiao,¹ W. B. Jiang,¹ Y. Chen,¹ F. Steglich,^{1,4} and H. Q. Yuan^{1,5,†}

¹Center for Correlated Matter and Department of Physics, Zhejiang University, Hangzhou 310058, China

²SEPnet and Hubbard Theory Consortium, University of Kent, Canterbury CT2 7NH, United Kingdom

³H. H. Wills Physics Laboratory, University of Bristol, Tyndall Avenue, Bristol BS8 1TL, United Kingdom

⁴Max Planck Institute for Chemical Physics of Solids, D-01187 Dresden, Germany

⁵Collaborative Innovation Center of Advanced Microstructures, Nanjing 210093, China

(Received 28 February 2016; published 7 July 2016)

The nature of the pairing states of superconducting LaNiC_2 and LaNiGa_2 has to date remained a puzzling question. Broken time reversal symmetry has been observed in both compounds and a group theoretical analysis implies a nonunitary triplet pairing state. However, all the allowed nonunitary triplet states have nodal gap functions but most thermodynamic and NMR measurements indicate fully gapped superconductivity in LaNiC_2 . Here we probe the gap symmetry of LaNiGa_2 by measuring the London penetration depth, specific heat, and upper critical field. These measurements demonstrate two-gap nodeless superconductivity in LaNiGa_2 , suggesting that this is a common feature of both compounds. These results allow us to propose a novel triplet superconducting state, where the pairing occurs between electrons of the same spin, but on different orbitals. In this case the superconducting wave function has a triplet spin component but isotropic even parity gap symmetry, yet the overall wave function remains antisymmetric under particle exchange. This model leads to a nodeless two-gap superconducting state which breaks time reversal symmetry, and therefore accounts well for the seemingly contradictory experimental results.

DOI: 10.1103/PhysRevLett.117.027001

The breaking of symmetries in addition to gauge symmetry upon entering the superconducting state usually indicates an unconventional order parameter. Several materials have been found to break time reversal symmetry (TRS) in the superconducting state through the detection of spontaneous magnetic fields below T_c using zero-field muon-spin relaxation (μSR). In some cases, such as Sr_2RuO_4 [1] and UPt_3 [2,3] where TRS breaking is also supported by measurements of the polar Kerr effect [4,5], there exists additional evidence for triplet superconductivity [6–9]. Recently, other superconductors have been reported to show TRS breaking, such as Re_6Zr [10] and $\text{Lu}_5\text{Rh}_6\text{Sn}_{18}$ [11], but there is not yet other evidence for unconventional superconductivity and fully gapped behavior is observed. In general the breaking of TRS does not necessarily imply triplet pairing and it is expected for some multiband singlet states such as $s + is$, where there is a phase difference between the gaps which is neither zero nor π [12]. However, a particular conundrum is presented by the TRS breaking in LaNiC_2 [13] and LaNiGa_2 [14], where it has been argued that as a result of the low symmetry of the orthorhombic crystal structures of both compounds, broken TRS necessarily implies nonunitary triplet superconductivity and all the TRS breaking states have nodes in the gap function [15]. Although evidence for nodal superconductivity was found recently from some measurements

[16,17], recent specific heat [18,19], nuclear quadrupole relaxation [20] and penetration depth [19] measurements indicate fully gapped behavior in LaNiC_2 . In addition, evidence for two-gap superconductivity was found from the specific heat, superfluid density, and upper critical field [19]. There have been fewer measurements of superconductivity in LaNiGa_2 [21], which has an orthorhombic centrosymmetric crystal structure in contrast to noncentrosymmetric LaNiC_2 , although fully gapped behavior was inferred from the specific heat [22].

In this Letter, we suggest a solution to this apparent contradiction from measurements of the London penetration depth, specific heat, and upper critical field, all of which consistently suggest the presence of two-gap superconductivity in LaNiGa_2 . Along with previous results for LaNiC_2 [19], we establish that nodeless, two-gap superconductivity is a common feature of these compounds. We propose that pairing between electrons with the same spins but on different orbitals gives rise to a triplet superconducting state with even parity pairing in both compounds, where the wave function remains antisymmetric overall due to a sign change upon exchanging electrons between different orbitals. Here additional lowering of the free energy is achieved by an additional field that splits the spin-up and spin-down Fermi surfaces, leading to two distinct gap values.

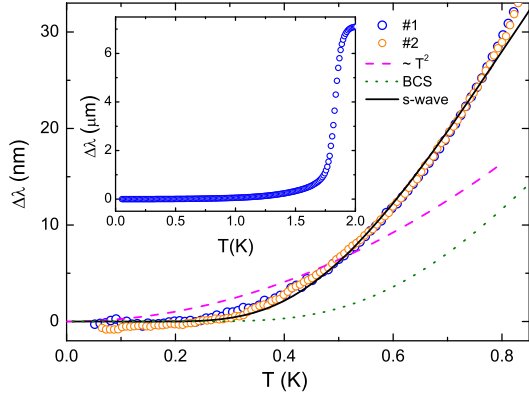


FIG. 1. London penetration depth $\Delta\lambda(T)$ of two samples of LaNiGa_2 at low temperatures. The solid and dashed lines show fits of $\Delta\lambda(T)$ to an s wave model with $\Delta(0) = 1.30k_B T_c$, and a T^2 dependence, respectively. The dotted line shows $\Delta\lambda(T)$ for an isotropic, weakly coupled BCS superconductor. The inset shows $\Delta\lambda(T)$ for sample No. 1 up to 2 K.

Polycrystalline LaNiGa_2 was prepared by arc melting stoichiometric quantities of La (99.98%), Ni (99.99%), and Ga (99.999%) in argon gas. The ingots were sealed in evacuated quartz tubes and annealed at 600 °C for one month. Powder x-ray diffraction measurements showed that the samples are single phase with lattice parameters consistent with previous results [22]. The residual resistivity of $\rho_0 \approx 1.6 \mu\Omega \text{ cm}$ and $RRR = \rho_{300 \text{ K}}/\rho_{4 \text{ K}} \approx 28$ indicate a high sample quality and a transition temperature $T_c \approx 1.8 \text{ K}$ was determined from the onset of a sharp superconducting transition. The ac magnetic susceptibility was measured in a ^3He cryostat and heat capacity measurements were performed using a Quantum Design Physical Property Measurement System. The London penetration depth was measured in a ^3He cryostat ($0.4 \text{ K} < T < 3 \text{ K}$) and a dilution refrigerator ($0.05 \text{ K} < T < 0.8 \text{ K}$) utilizing a tunnel diode oscillator (TDO) based technique, where the change of the London penetration depth is proportional to the TDO frequency shift, i.e., $\Delta\lambda(T) = \lambda(T) - \lambda_0 = G\Delta f(T)$, where λ_0 is the zero temperature penetration depth and G is determined by the coil and sample geometry [23].

Figure 1 shows $\Delta\lambda(T)$ for two samples of LaNiGa_2 , where G is 5.2 \AA/Hz and 11.6 \AA/Hz for samples No. 1 and No. 2, respectively. The inset displays $\Delta\lambda(T)$ from 2 K down to 0.05 K for sample No. 1. The signal drops abruptly around the transition temperature $T_c = 1.8 \text{ K}$, which is consistent with the T_c from resistivity (not shown) and ac susceptibility measurements (inset of Fig. 4). The low temperature data of $\Delta\lambda(T)$ are displayed in the main panel of Fig. 1. For nodal superconductors at low temperatures, $\Delta\lambda(T) \sim T^n$ with $n = 1$ for line nodes and $n = 2$ for point nodes. Our data does not display this behavior and the flattening of $\Delta\lambda(T)$ indicates nodeless superconductivity. For isotropic s wave superconductors at $T \ll T_c$, $\Delta\lambda = \lambda_0 \sqrt{\pi\Delta(0)/2k_B T} \exp[-\Delta(0)/k_B T]$, where $\Delta(0)$ is the zero temperature gap amplitude. As shown by the solid line in

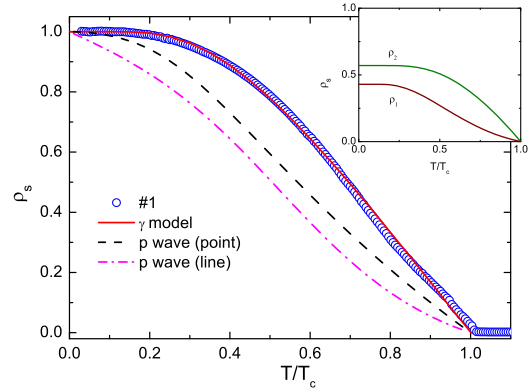


FIG. 2. Superfluid density $\rho_s(T)$ against T/T_c . The solid line shows the fitted two-band model, while the dashed and dashed-dotted lines show models with point and line nodes, respectively. The inset shows the components of the two-band model.

Fig. 1, the data are well fitted by this expression at low temperatures. The fitted gap of $\Delta(0) = 1.30k_B T_c$ is significantly smaller than the weakly coupled BCS value of $1.76k_B T_c$, indicating either multiple gaps or gap anisotropy. The behavior of $\Delta\lambda(T)$ for such a BCS model (dotted line) shows poor agreement.

To further analyze the gap symmetry of LaNiGa_2 , we calculated the superfluid density using $\rho_s(T) = [\lambda_0/\lambda(T)]^2$, where $\lambda_0 = 350 \text{ nm}$ [14]. Figure 2 shows $\rho_s(T)$ for sample No. 1 where the flat behavior at low temperatures again indicates fully gapped superconductivity. The superfluid density is shown for two nodal gap structures which cannot account for the data, with point nodes where $\Delta_k = \Delta(T) \sin(\theta)$ (dotted line) and with line nodes where $\Delta_k = \Delta(T) \cos(\theta)$ (dashed-dotted line). Here $\Delta(T)$ is the gap temperature dependence from Ref. [24] with $\Delta(0) = 1.6k_B T_c$ and $3.5k_B T_c$ for the respective models. The presence of multiple electron and hole Fermi surface sheets revealed by band structure calculations [25,26], as well as a gap significantly smaller than the BCS value derived from fitting $\Delta\lambda(T)$ at low temperatures, suggest the possibility of multigap superconductivity. Therefore the data are analyzed using a two-band γ model [27], where the gap on each band is calculated self-consistently. The parameters are the partial density of states n_1 and n_2 , the intraband pairing potentials λ_{11} and λ_{22} along with λ_{12} and λ_{21} which characterize the interband coupling. The superfluid density of a two-band superconductor can be summarized as $\rho_s(T) = x\rho_1(T) + (1-x)\rho_2(T)$, where $\rho_i(T)$ is the single band superfluid density for the gap $\Delta_i(T)$ ($i = 1, 2$) and x is the relative weight of $\rho_1(T)$ [24]. When using this procedure with $\lambda_{12} = \lambda_{21}$, the free parameters are n_1 , λ_{11} , λ_{12} , λ_{22} and x . We obtain a good fit across the whole temperature range with the best fitting parameters of $n_1 = 0.4$, $\lambda_{11} = 0.25$, $\lambda_{22} = 0.153$, $\lambda_{12} = 0.016$, and $x = 0.43$. The value of x is close to n_1 , suggesting the Fermi velocities of each band are similar. The fit to the γ model is shown by the solid line in Fig. 2 and the zero temperature gaps are

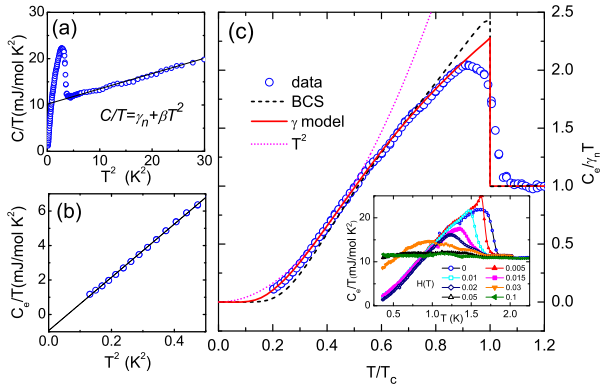


FIG. 3. (a) Specific heat C/T against T^2 for LaNiGa₂. The solid line shows a linear fit above T_c . (b) The electronic specific heat C_e/T against T^2 at low temperatures. The solid line shows a linear fit which extrapolates to negative C_e/T . (c) Temperature dependence of C_e/T , normalized to the normal state value. The solid line shows the γ model fit, while the dashed and dotted lines show the behavior of a weakly coupled, isotropic BCS superconductor and a T^2 dependence, respectively. The inset shows $C_e/T(T)$ in various applied magnetic fields.

$\Delta_1(0) = 1.29k_B T_c$ and $\Delta_2(0) = 2.04k_B T_c$. The smaller gap agrees well with $\Delta(0) = 1.30k_B T_c$ obtained from fitting $\Delta\lambda(T)$ (Fig. 1), as expected for two-band superconductors [28].

Specific heat (C) results for LaNiGa₂ are shown in Fig. 3(a), where C/T follows a T^2 dependence above T_c . The normal state is fitted with $C/T = \gamma_n + \beta T^2$, giving a Sommerfeld coefficient $\gamma_n = 10.54$ mJ/mol K² and a Debye temperature $\Theta_D = 294$ K from the phonon contribution βT^2 , consistent with previous results [22]. The electronic specific heat (C_e) is obtained by subtracting the phonon term, and $C_e(T)/\gamma_n T_c$ is displayed in Fig. 3(c). The dashed line shows the specific heat of an isotropic, weakly coupled BCS superconductor, which also deviates from the data. Although $C_e(T)/T$ is not saturated down to 0.35 K, this is consistent with the penetration depth results, which only become flat below about 0.25 K. While $C_e(T)/T$ shows quadraticlike behavior at low temperatures [Fig. 3(b)], a negative value of $C_e(0)/T = -0.93$ mJ/mol K² is obtained upon extrapolating to zero temperature, suggesting a nodeless superconducting gap. $C_e(T)/T$ in the superconducting state is fitted using a two-band model [29], $C_e(T)/T = x C_e^{\Delta_1}(T)/T + (1-x) C_e^{\Delta_2}(T)/T$, where $C_e^{\Delta_i}(T)/T$ is the single band $C_e(T)$ with a gap $\Delta_i(T)$, calculated using the same expression as for the superfluid density fitting. From Fig. 3(c), it can be seen that the data are well described by this model with fitted parameters $n_1 = 0.4$, $\lambda_{11} = 0.261$, $\lambda_{22} = 0.149$, $\lambda_{12} = 0.02$, and $x = 0.31$. The derived specific heat jump is $\Delta C/\gamma T_c = 1.28$ and the gap values at zero temperature are $\Delta_1(0) = 1.08k_B T_c$ and $\Delta_2(0) = 2.06k_B T_c$. This demonstrates that the specific heat measurements are consistent with two-gap superconductivity, as deduced from the superfluid density fitting.

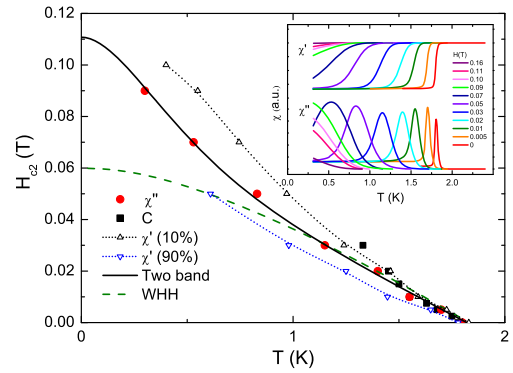


FIG. 4. Upper critical field $H_{c2}(T)$ of LaNiGa₂ from specific heat and ac susceptibility measurements. For the ac susceptibility, $H_{c2}(T)$ were obtained from the peak in χ'' , as well as where χ' reaches 10% and 90% of full screening, while the midpoint of the transition was used for the values from specific heat measurements. The solid and dashed lines show the two-band and WHH models, respectively, while the dotted lines are guides for the eye. The inset shows the real and imaginary parts of the ac susceptibility $\chi(T)$ in various fields.

To determine the upper critical field [$H_{c2}(T)$] of LaNiGa₂, we measured the ac susceptibility χ (inset of Fig. 4) and specific heat [inset of Fig. 3(c)] in various magnetic fields. A transition cannot be clearly resolved in the specific heat data for applied fields greater than 0.03 T, the reason for which is not clear and requires further studies. As shown in Fig. 4, $H_{c2}(T)$ is almost linear near T_c . However, the curvature of $H_{c2}(T)$ shows a clear upturn at low temperatures, deviating from the Werthamer-Helfand-Hohenberg (WHH) model (dashed line) [30]. Such a negative curvature of $H_{c2}(T)$ is a common feature of multiband superconductivity. For a multiband system taking into account both interband and intraband couplings, $H_{c2}(T)$ can be calculated following Ref. [31]. The upper critical field was fitted with the same parameters used to fit the superfluid density, so that the only free parameters were the diffusivities of the bands (D_1 and D_2). The data are well fitted by the model (solid line in Fig. 4) and therefore $H_{c2}(T)$ agrees well with two-band superconductivity. The obtained value of D_2/D_1 is 0.15, while the extrapolated zero-temperature upper critical field is $\mu_0 H_{c2}(0) \approx 0.11$ T.

Therefore measurements of the penetration depth, specific heat, and upper critical field consistently support nodeless two-gap superconductivity in LaNiGa₂. Two-gap behavior was also observed in LaNiC₂ [19], suggesting that nodeless, two-gap superconductivity is another common feature of these compounds, in addition to TRS breaking. In what follows we propose a unified view of these materials in which the two phenomena have a common origin.

Significant differences exist between the two materials. Electronic structure calculations reveal that either one or two bands cross the Fermi level (E_F) in LaNiC₂ [32,33], while LaNiGa₂ has a very different Fermi surface, with several bands at E_F [25,26]. Moreover, whereas the crystal

structure of LaNiGa₂ has a center of inversion, that of LaNiC₂ lacks it. As a result, in LaNiC₂ the spin-orbit coupling may lead to a superconducting state which is a mixture of spin singlet and spin triplet [34–36]. In contrast, for LaNiGa₂ such a state is forbidden by symmetry.

Several works have discussed LaNiC₂ and LaNiGa₂ in terms of a conventional BCS pairing mechanism [25,26,33,37] and this scenario leads to fully gapped superconductivity with two-gap behavior arising from the involvement of two distinct bands. However, such theories are not readily reconciled with the observation of TRS breaking in both compounds [13,14]. To address this, it was proposed that in LaNiC₂ the broken TRS may arise from a small admixture of triplet pairing to an otherwise largely conventional superconducting order parameter [33]. Alternatively, it was hypothesized that a nontrivial phase factor between the *s* wave gaps in two different bands (an *s* + *is* state) might be responsible for broken TRS [25]. However, the point groups of the crystal structures of LaNiC₂ and LaNiGa₂ are *C*_{2*v*} and *D*_{2*h*}, respectively, both of which only have one-dimensional irreducible representations [13,14] whereas a multidimensional order parameter is required to break TRS at *T*_{*c*} [38]. In the triplet admixture scenario, the relevant point group is the double group *C*_{2*v*,*J*} whose irreducible representations have the same dimensionality as those of *C*_{2*v*}. In the *s* + *is* scenario, the point group is either *C*_{2*v*} or *D*_{2*h*}, if the bands are strongly coupled, or the products *C*_{2*v*} ⊗ *C*_{2*v*} or *D*_{2*h*} ⊗ *D*_{2*h*}, if they are decoupled, which also only have one-dimensional irreducible representations. Thus in either scenario the broken TRS would require a first-order transition or multiple superconducting phase transitions [15,39]. While the latter has been observed in UPt₃ [40], there is no experimental evidence in these compounds.

In the case of weak spin-orbit coupling the relevant point groups for LaNiC₂ and LaNiGa₂ are *C*_{2*v*} ⊗ *SO*(3) and *D*_{2*h*} ⊗ *SO*(3), respectively, both of which have three-dimensional irreducible representations and there are four TRS-breaking superconducting instabilities [13–15], all of them in the purely triplet channel and thus in stark contrast to the above scenarios. All four instabilities correspond to nonunitary (equal-spin) pairing, for which we expect an additional, subdominant order parameter, in the form of a bulk magnetization appearing below *T*_{*c*}, which may have been observed in LaNiC₂ [41]. However, all of these nonunitary triplet states have nodal gap functions, which is clearly inconsistent with this work and Ref. [19].

As a result, we suggest that a new mechanism may be present in these materials. An isotropic gap which does not change sign can result from an on-site interaction, which is not possible for equal spin pairing in a single-orbital model, but could result from a local attraction between electrons with equal spins on different orbitals. The pairing potential has the form $\Delta_{\alpha,\beta}^{n,m}(\mathbf{k})$, where *n*, *m* are orbital indices and α , β are the spin indices of the two paired electrons. For an isotropic gap with the formation of Cooper pairs within one

orbital, $\Delta_{\alpha,\beta}^{n,m}(\mathbf{k}) = \Delta_{\alpha,\beta}^{n,n}$ and therefore to keep the gap function antisymmetric under the exchange of two fermions, it is necessary that $\Delta_{\alpha,\beta}^{n,m} = -\Delta_{\beta,\alpha}^{n,m}$, that is there is singlet pairing between electrons of opposite spins. However, if the pairing occurs between electrons on different orbitals, the condition for triplet pairing $\Delta_{\alpha,\beta}^{n,m} = \Delta_{\beta,\alpha}^{n,m}$ can be met if $\Delta_{\alpha,\beta}^{n,m} = -\Delta_{\alpha,\beta}^{m,n}$, that is the change of signs is achieved through an antisymmetric orbital index. Similar scenarios have been proposed to make *d* wave pairing and fully gapped behavior compatible in the iron pnictides [42] and to propose fully gapped triplet pairing in that same family of materials [43]. Our approach generalizes the work of Ref. [43] to the nonunitary case, allowing for broken TRS.

The simplest theory embodying the above ideas features an electron-electron interaction $\hat{V} = -U \sum_{j,\sigma} c_{Aj\sigma}^\dagger c_{Bj\sigma}^\dagger c_{Bj\sigma} c_{Aj\sigma}$. Here $c_{Aj\sigma}^\dagger$ creates an electron in an *A* orbital on the *j*th lattice site with spin index σ . \hat{V} describes attraction, of strength *U*, between two electrons with parallel spins that occupy different orbitals *A*, *B* on the same site *j*. Within a standard variational mean field theory, the effect of \hat{V} can be described by two mean fields $\Delta_{\uparrow\uparrow} c_{Aj\uparrow}^\dagger c_{Bj\uparrow}^\dagger + \Delta_{\downarrow\downarrow} c_{Aj\downarrow}^\dagger c_{Bj\downarrow}^\dagger + \text{H.c.}$ and $\Phi_{A\sigma} c_{Aj\sigma}^\dagger c_{Aj\sigma} + \Phi_{B\sigma} c_{Bj\sigma}^\dagger c_{Bj\sigma}$. $\Delta_{\uparrow\uparrow}$ and $\Delta_{\downarrow\downarrow}$ describe uniform, equal-spin pairing between an electron in an *A* orbital and an electron in a *B* orbital on the same site. Our pairing potentials correspond to the Δ_1 and Δ_{-1} terms in Ref. [43], while we do not include the Δ_0 term. The additional mean field $\Phi_{n\sigma}$ takes care of the spontaneous spin polarization [14,44].

Diagonalizing the Bogoliubov–de Gennes equations yields low-energy quasiparticles which have a well-defined spin index σ but mixed orbital character. For each value of the spin, the quasiparticle spectrum has four branches and depends on the details of the splitting between the *A* and *B* orbital energy levels and band hybridizations. Neglecting these, it simplifies to two doubly degenerate branches $E_\sigma = \pm \sqrt{(\epsilon - \mu + \Phi_\sigma)^2 + |\Delta_{\sigma\sigma}|^2}$, which yields two fully open gaps of different sizes for $\uparrow\uparrow$ and $\downarrow\downarrow$ pairing. Such a simple model is consistent with electronic structure calculations of LaNiGa₂, which reveal the presence of two pairs of Fermi surface sheets, which are in close proximity in the Brillouin zone [26]. The details of the derivation and more general expressions will be provided elsewhere. Spectroscopically, this could be very similar to the conventional two-band behavior captured by the γ -model used to fit our data. However, note that the two values of the gap are associated with two different values of the spin, rather than two band indices.

Further hints of an unconventional pairing mechanism come from recent measurements of LaNiC₂ under pressure, which reveal a broad superconducting dome, where the maximum of *T*_{*c*} coincides with a crossover from a metallic normal state to one with strongly correlated electronic interactions [45]. One possibility is that fluctuations of the correlated state mediate the pairing interaction, which

might then look different from the simple, on-site form used above. Alternatively, the local attraction between equal spins could result from Hund's rules. Furthermore, our theory provides a mechanism for an on-site attraction leading to triplet pairing, suggesting the possibility of TRS breaking superconductivity mediated by phonons.

To summarize, we performed measurements of London penetration depth, specific heat, and upper critical field which show two-gap, nodeless superconductivity in LaNiGa_2 . The presence of two gaps in both LaNiGa_2 and LaNiC_2 allows us to propose a novel nonunitary triplet state, where the gap symmetry has even parity. This can reconcile the observation of fully gapped behavior and the breaking of TRS in both compounds and further work is required to elucidate the mechanism which leads to this novel pairing state.

This work was supported by the National Natural Science Foundation of China (No. 11474251), the Science Challenge Program of China, the National Basic Research Program of China (No. 2016YFA0300202) and the Max Planck Society under the auspices of the Max Planck Partner Group of the MPI for Chemical Physics of Solids, Dresden.

*msmidman@zju.edu.cn

†hgyuan@zju.edu.cn

- [1] G. M. Luke *et al.*, *Nature (London)* **394**, 558 (1998).
- [2] G. M. Luke, A. Keren, L. P. Le, W. D. Wu, Y. J. Uemura, D. A. Bonn, L. Taillefer, and J. D. Garrett, *Phys. Rev. Lett.* **71**, 1466 (1993).
- [3] P. de R otier, A. Huxley, A. Yaouanc, J. Flouquet, P. Bonville, P. Imbert, P. Pari, P. C. M. Gubbens, and A. M. Mulders, *Phys. Lett. A* **205**, 239 (1995).
- [4] J. Xia, Y. Maeno, P. T. Beyersdorf, M. M. Fejer, and A. Kapitulnik, *Phys. Rev. Lett.* **97**, 167002 (2006).
- [5] E. R. Schemm, W. J. Gannon, C. M. Wishne, W. P. Halperin, and A. Kapitulnik, *Science* **345**, 190 (2014).
- [6] K. Ishida, H. Mukuda, Y. Kitaoka, K. Asayama, Z. Q. Mao, Y. Mori, and Y. Maeno, *Nature (London)* **396**, 658 (1998).
- [7] A. Mackenzie and Y. Maeno, *Rev. Mod. Phys.* **75**, 657 (2003).
- [8] R. Joynt and L. Taillefer, *Rev. Mod. Phys.* **74**, 235 (2002).
- [9] H. Tou, Y. Kitaoka, K. Ishida, K. Asayama, N. Kimura, Y.  onuki, E. Yamamoto, Y. Haga, and K. Maezawa, *Phys. Rev. Lett.* **80**, 3129 (1998).
- [10] R. P. Singh, A. D. Hillier, B. Mazidian, J. Quintanilla, J. F. Annett, D. M. Paul, G. Balakrishnan, and M. R. Lees, *Phys. Rev. Lett.* **112**, 107002 (2014).
- [11] A. Bhattacharyya, D. T. Adroja, J. Quintanilla, A. D. Hillier, N. Kase, A. M. Strydom, and J. Akimitsu, *Phys. Rev. B* **91**, 060503(R) (2015).
- [12] D. F. Agterberg, V. Barzykin, and L. P. Gor'kov, *Phys. Rev. B* **60**, 14868 (1999).
- [13] A. D. Hillier, J. Quintanilla, and R. Cywinski, *Phys. Rev. Lett.* **102**, 117007 (2009).
- [14] A. D. Hillier, J. Quintanilla, B. Mazidian, J. F. Annett, and R. Cywinski, *Phys. Rev. Lett.* **109**, 097001 (2012).
- [15] J. Quintanilla, A. D. Hillier, J. F. Annett, and R. Cywinski, *Phys. Rev. B* **82**, 174511 (2010).
- [16] W. H. Lee, H. K. Zeng, Y. D. Yao, and Y. Y. Chen, *Physica (Amsterdam)* **266C**, 138 (1996).
- [17] I. Bonalde, R. L. Ribeiro, K. J. Syu, H. H. Sung, and W. H. Lee, *New J. Phys.* **13**, 123022 (2011).
- [18] V. K. Pecharsky, L. L. Miller, and K. A. Gschneidner, *Phys. Rev. B* **58**, 497 (1998).
- [19] J. Chen, L. Jiao, J. L. Zhang, Y. Chen, L. Yang, M. Nicklas, F. Steglich, and H. Q. Yuan, *New J. Phys.* **15**, 053005 (2013).
- [20] Y. Iwamoto, Y. Iwasaki, K. Ueda, and T. Kohara, *Phys. Lett. A* **250**, 439 (1998).
- [21] Y. Aoki, K. Terayama, and H. Sato, *J. Phys. Soc. Jpn* **64**, 3986 (1995).
- [22] N. L. Zeng and W. H. Lee, *Phys. Rev. B* **66**, 092503 (2002).
- [23] R. Prozorov, R. W. Giannetta, A. Carrington, and F. M. Araujo-Moreira, *Phys. Rev. B* **62**, 115 (2000).
- [24] R. Prozorov and R. W. Giannetta, *Supercond. Sci. Technol.* **19**, R41 (2006).
- [25] I. Hase and T. Yanagisawa, *J. Phys. Soc. Jpn.* **81**, 103704 (2012).
- [26] D. Singh, *Phys. Rev. B* **86**, 174507 (2012).
- [27] V. G. Kogan, C. Martin, and R. Prozorov, *Phys. Rev. B* **80**, 014507 (2009).
- [28] M. Zehetmayer, *Supercond. Sci. Technol.* **26**, 043001 (2013).
- [29] F. Bouquet, Y. Wang, R. A. Fisher, D. G. Hinks, J. D. Jorgenson, A. Junod, and N. E. Phillips, *Europhys. Lett.* **56**, 856 (2001).
- [30] N. Werthamer, E. Helfand, and P. Hohenberg, *Phys. Rev.* **147**, 295 (1966).
- [31] A. Gurevich, *Phys. Rev. B* **67**, 184515 (2003).
- [32] I. Hase and T. Yanagisawa, *J. Phys. Soc. Jpn* **78**, 084724 (2009).
- [33] A. Subedi and D. J. Singh, *Phys. Rev. B* **80**, 092506 (2009).
- [34] L. P. Gor'kov and E. I. Rashba, *Phys. Rev. Lett.* **87**, 037004 (2001).
- [35] P. A. Frigeri, D. F. Agterberg, A. Koga, and M. Sigrist, *Phys. Rev. Lett.* **92**, 097001 (2004).
- [36] H. Q. Yuan, D. F. Agterberg, N. Hayashi, P. Badica, D. Vandervelde, K. Togano, M. Sigrist, and M. B. Salamon, *Phys. Rev. Lett.* **97**, 017006 (2006).
- [37] H. M. T ut nc u and G. P. Srivastava, *Appl. Phys. Lett.* **104**, 022603 (2014).
- [38] M. Sigrist, *Physica (Amsterdam)* **341–348C**, 695 (2000).
- [39] B. Mettout, P. Tol dano, and V. Lorman, *Phys. Rev. Lett.* **77**, 2284 (1996).
- [40] R. A. Fisher, S. Kim, B. F. Woodfield, N. E. Phillips, L. Taillefer, K. Hasselbach, J. Flouquet, A. L. Giorgi, and J. L. Smith, *Phys. Rev. Lett.* **62**, 1411 (1989).
- [41] A. Sumiyama, D. Kawakatsu, J. Gouchi, A. Yamaguchi, G. Motoyama, Y. Hirose, R. Settai, and Y.  onuki, *J. Phys. Soc. Jpn* **84**, 013702 (2015).
- [42] T. Tzen Ong, P. Coleman, and J. Schmalian, *Proc. Natl. Acad. Sci. U.S.A.* **113**, 5486 (2016).
- [43] X. Dai, Z. Fang, Y. Zhou, and F.-C. Zhang, *Phys. Rev. Lett.* **101**, 057008 (2008).
- [44] K. Miyake, *J. Phys. Soc. Jpn* **83**, 053701 (2014).
- [45] S. Katano, H. Nakagawa, K. Matsubayashi, Y. Uwatoko, H. Soeda, T. Tomita, and H. Takahashi, *Phys. Rev. B* **90**, 220508(R) (2014).